24th ABCM International Congress of Mechanical Engineering
December 3-8, 2017, Curitiba, PR, Brazil

COBEM-2017-1379
OWC SIMULATION COMPARISION BETWEEN TURBULENT AND LAMINAR MODELS USING OPENFOAM CODE

Andrei Luís Garcia Santos
Dante Vinícius Eloy Barbosa
Jeferson Avila Souza
Elizaldo Domingues dos Santos
Escola de Engenharia (EE), Universidade Federal do Rio Grande (FURG) – Avenida Itália, km 8 – C.P. 474 – Rio Grande - RS
andrei_eng_mec@hotmail.com, dante_barbosa@yahoo.com.br, jasouza1974@gmail.com, elizaldodossantos@gmail.com

Abstract. *Wave energy has been widely studied in the field of computational modeling generating observations in several fields of research. Oscillating Water Column (OWC) devices have been studied in the search for results that can be used as a recommendation for chamber and turbine design. Main goal is to obtain the best possible performance in the transformation of wave energy into electrical energy. Wave motion and water iteration with the device are simulated with Computational Fluid Dynamics (CFD) codes. Usually, laminar models are used and just a few works include turbulence in the simulation. In this sense, present work compares laminar and turbulent simulations aiming to determine best way to simulate this type of problem. Preliminary comparisons for velocity vectors and magnitude have shown that k-ω turbulent model presents greater difference results in relation all other models studied (k-ε and Spalart Allmaras).*

Keywords: *Wave energy, OWC, OpenFoam, Turbulence models.*

1. INTRODUCTION

It is well known that electricity is the most prominent energy modality in the human existence, since it is inserted in almost all existing now-a-days technologies.

According to (Thorpe, 1999), there are two energy sources: renewable and non-renewable. Both are capable of transforming different forms of energy into electricity. Non-renewable sources are represented by nuclear energy and fossil fuels, which are the most widely used nowadays because their are ease to extract and less expensive. On the other hand, the scarcity of non-renewable resources, as well as the great environmental impact generated by them, motivates several studies for the use of renewable energy sources, among which we can highlight: biomass, wind power, solar energy and wave energy.

In this sense, the energy of the oceans has been studied to be part of the world energy matrix, since it is an abundant and inexhaustible source. The oceans contain a potential of about 10 TW, which compares to entire current consumption of electrical energy across the globe.

In this work, the focus of the study is a simulation of an OWC device (Oscillating Water Column) in a wave tank, with laminar and turbulent flow regimes, using OpenFOAM software and aiming to evaluate the differences in solutions.

2. COMPUTATIONAL PROCEDURE

A first test is performed in a tank without the OWC device. Tank geometry is shown in Fig. 1, where H_T is the tank height [m], h is the water depth and L is the tank length.

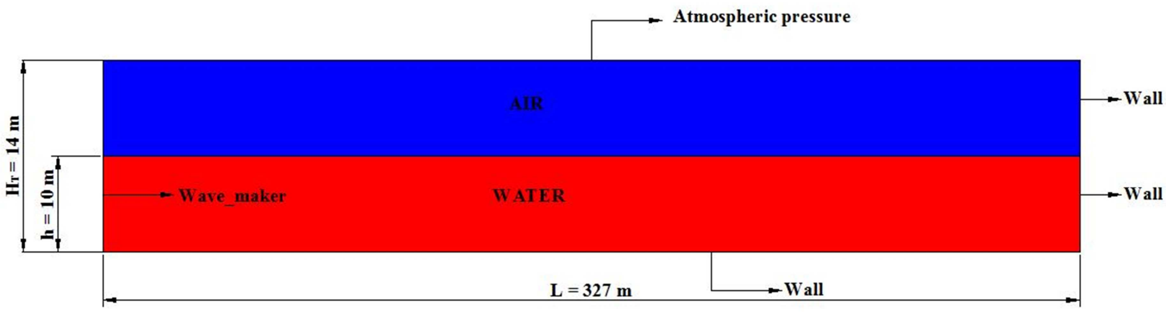

Figure 1. Wave tank geometry and boundary conditions

For all simulations in this work, OpenFOAM (*Ramim, et al.,2001)*- Open Field Operation Manipulation - software was used. It's a free open source CFD program, written in C++. Incompressible, unsteady, two-phases *interFoam* solver has been used to solve both laminar and turbulent flows. It uses the Volume of Fluid (VOF) formulation and solves three-dimensional continuity, momentum and volume fraction governing equations (Eqs. 1, to 3).

$$\nabla \cdot \mathrm{U} = 0 \tag{1}$$

$$\frac{\partial \rho U}{\partial t} + \nabla \cdot (\rho U U) - \nabla \cdot (\mu \nabla U) = -\nabla p' - g \cdot X \nabla \rho + \nabla U \cdot \nabla \mu + \sigma k \nabla \alpha \tag{2}$$

$$\frac{\partial \alpha}{\partial t} + \nabla \cdot U\alpha + \nabla \cdot U_r \alpha(1-\alpha) = 0 \tag{3}$$

where, U_r is the relative velocity among the fluids, given:

$$U_r = \min(calpha|U|, max|U|) \tag{4}$$

In Eqs. 1 to 3, **U** is velocity vector [m/s]; **g** is gravity acceleration [m/s²]; **ρ** is density [kg/m³]; **μ** is dynamic viscosity [Pa s]; **p'** is pseudo-dynamic pressure [Pa]; **X** is the position vector [m]; **σ** is surface tension coefficient; **k** is the curvature of the interface and **α** is the water's volume fraction. Average viscosity and density are given by Eqs. 5 and 6:

$$\mu = \alpha \mu_{water} + (1-\alpha)\mu_{air} \tag{5}$$

$$\rho = \alpha \rho_{water} + (1-\alpha)\rho_{air} \tag{6}$$

Boundary conditions for the problem are shown in Fig. 1. According Dean and Dalrymple (1991), prescribed velocity applied to the wave maker (in the x and z directions) is given by:

$$u = \frac{Hgk\cosh[k(h+z)]}{2\sigma\cosh(kh)}\cos(kx-\sigma t) + \frac{3\,H^2\sigma k\cosh[2k(h+z)]}{16 sinh^4(kh)}\cos[2(kx-\sigma t)] \tag{7}$$

$$w = \frac{Hgk\sinh[k(h+z)]}{2\sigma\cosh(kh)}\sin(kx-\sigma t) + \frac{3H^2\sigma k\sinh[2k(h+z)]}{16\, sinh^4(kh)}\sin[2(kx-\sigma t)] \tag{8}$$

The water raising surface is given by Eq. 9:

$$\eta = A\cos(kx-\omega t) \tag{9}$$

where, A is the wave amplitude [m], $k = 2\pi/l$ is the wave number [m^{-1}], $\omega = 2\pi/T$ is the angular frequency [s^{-1}], T the wave period [s], l the wave length [m] and t is the time [s]

2.1 Turbulence models

In this work, three simulations using different turbulent models were used to compare with another simulation using the laminar model. These were: *k-ε, k-ω and Spalart-Allmaras*. These three are classified as *RANS* models (Reynolds Averaged Navier-Stokes).

According (Launder et al., 1974; Henk et al.,2007 and FERRAZ et al., 2015), for *k-ε* and *k-ω* models the turbulent viscosity is given by Eqs. 10 and 11:

$$\upsilon_t = C_\mu \frac{k^2}{\varepsilon} \tag{10}$$

$$\upsilon_t = \alpha^* \frac{k}{\omega} \tag{11}$$

where, C_μ = 0.09 and α* is the coefficient that dampens the turbulent viscosity by making a low Reynolds number correction. The kinetic energy equation of turbulence, expressed by "*k*", and solved for both models is given by:

$$\frac{\partial k}{\partial t} + \bar{v}_j \frac{\partial k}{\partial x_j} = \tau_{ij} \frac{\partial \bar{v}_i}{\partial x_j} + \frac{\partial}{\partial x_j}\left[\left(\upsilon + \frac{\upsilon_t}{\sigma_k}\right)\frac{\partial k}{\partial x_j}\right] - \varepsilon \tag{12}$$

The the kinetic energy dissipation equation, "ε", for k-ε model is solved by:

$$\frac{\partial \varepsilon}{\partial t} + \bar{v}_j \frac{\partial \varepsilon}{\partial x_j} = \frac{\partial}{\partial x_j}\left[\left(\upsilon + \frac{\upsilon_t}{\sigma_\varepsilon}\right)\frac{\partial \varepsilon}{\partial x_j}\right] + C_{\varepsilon 1}\frac{\varepsilon}{k}\tau_{ij}\frac{\partial \bar{v}_i}{\partial x_j} - C_{\varepsilon 2}\frac{\varepsilon^2}{k} \tag{13}$$

where, $C_{\varepsilon 1}$ = 1.44, $C_{\varepsilon 2}$ =1.92, σ_k =1.0 and σ_ε =1.3.

In turn, the specific rate of turbulent kinetic energy equation, "ω", for k-ω model is represented by Eq. 14:

$$\frac{\partial \omega}{\partial t} + \bar{v}_j \frac{\partial \omega}{\partial x_j} = \frac{\partial}{\partial x_j}\left[\left(\upsilon + \frac{\upsilon_t}{\sigma_\omega}\right)\frac{\partial \omega}{\partial x_j}\right] + G_\omega - Y_\omega \tag{14}$$

where, σ_k = 2.0, σ_ω = 2.0 and the terms G_ω and Y_ω are, respectively, the generation and the dissipation of "ω".

In Spalart Allmaras model, the one equation to solve for $\tilde{v}$ variable, is shown in Eq. 15:

$$\frac{\partial \tilde{v}}{\partial t} + \frac{\partial \tilde{v}}{\partial x_i} u_i = G_v + \frac{1}{\sigma_{\tilde{v}}}\left[\frac{\partial}{\partial x_j}\left\{(\upsilon + \tilde{v})\frac{\partial \tilde{v}}{\partial x_j}\right\} + C_{b2}\left(\frac{\partial \tilde{v}}{\partial x_j}\right)^2\right] - Y_v \tag{15}$$

where, $\tilde{v}$ is the turbulent kinematic viscosity except near the wall regions, where a wall function is employed to take into account the anisotropy of the flow in that region. G_v is the turbulent viscosity production, $\sigma_{\tilde{v}}$ = 2/3 and C_{b2} = 0.622 are the model constants.

3. RESULTS AND DISCUSSION

At first, a grid refinement test was performed for a wave depth analytical verification for an empty OWC device tank. Figure 2 shows water elevation at x = 100 m (referred to Fig. 1). Maximum difference observed at the analytical's wave crest and the 426885 cells grid simulation was 3.86%. This result was calculated by the difference between the water raising surfaces in each simulation's time.

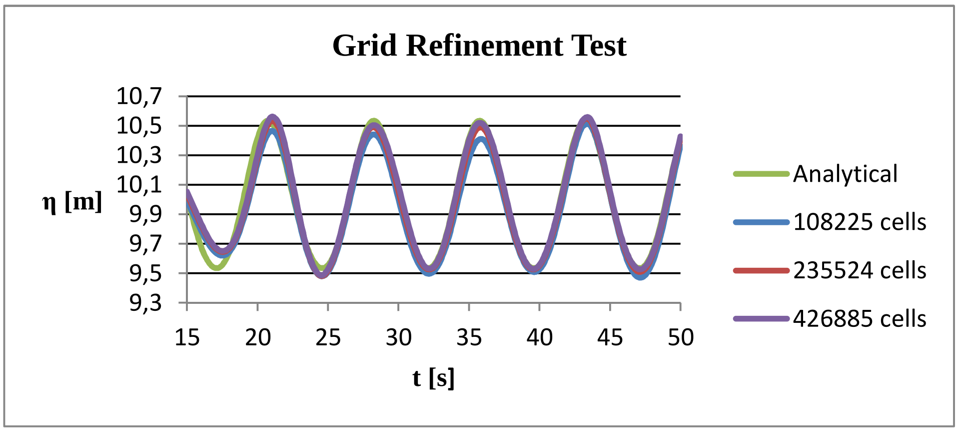

Figure 2. Grid Refinement Test.

Simulations were then performed in a tank with OWC device, where water depth was measured in the chamber device central region, shown in Fig. 3. Figure 3 shows only the region close to the device.

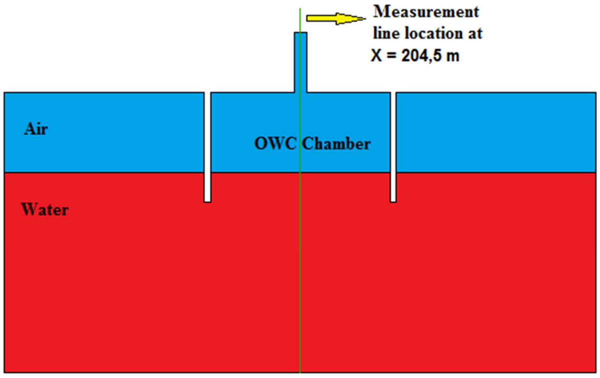

Figure 3. Tank with OWC device at x = 200 m and depth measurement line at x = 204.5 m.

With this configuration, the depth measured in the range of 18 to 52 s, for laminar and turbulent flows regimes, is shown in Figs. 4, 5 and 6:

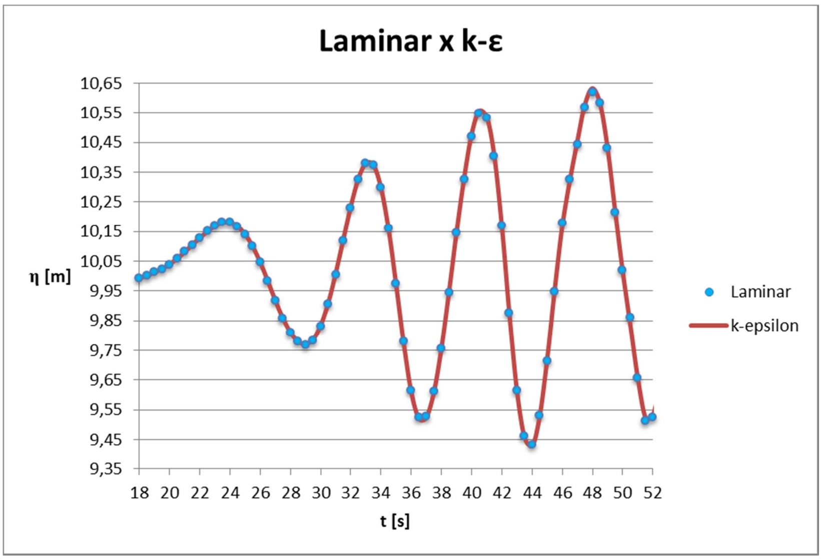

Figure 4. Comparison between laminar regime flow and turbulent k-ε model.

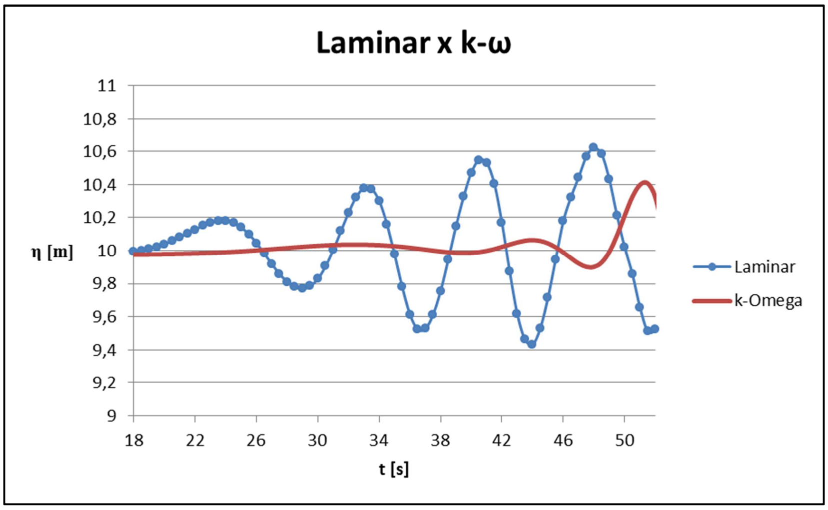

Figure 5. Comparison between laminar regime flow and turbulent k-ω model.

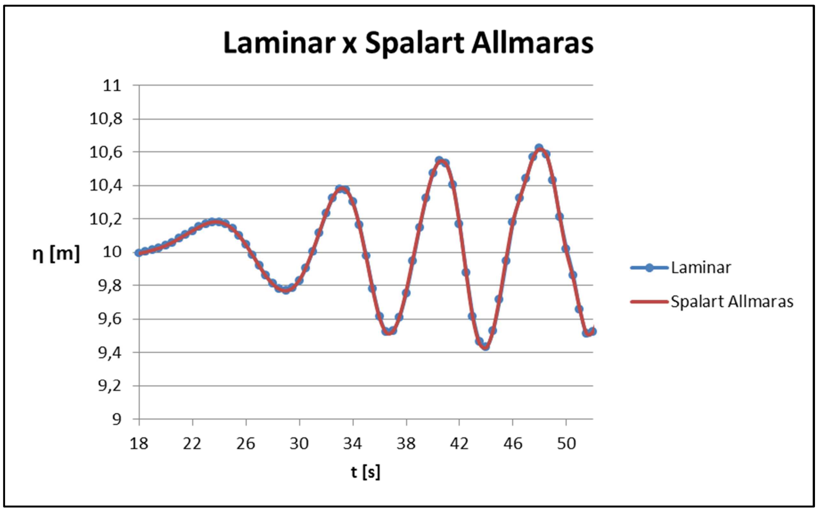

Figure 6. Comparison between laminar regime flow and turbulent Spalart Allmaras model.

In figures 4 to 6, it can be observed that the k-ω model presents the most discrepant results in relation to the laminar model. From what can be seen, this model presents the first highest water raising surface with 50 seconds of wave progression, while all other models have shown same results with 32 seconds. Table 1 shows the average difference error of each model in relation to the laminar model:

Table 1. Mean relative errors between turbulence models and laminar model for water raising free surface.

Turbulent Model	Error
k-ε	1.17%
k-ω	29.08%
Spalart Allmaras	0.61%

Figures 7 and 8 show, respectively, the velocity vector field for each simulated models and their velocity magnitude at the moment of highest water raising surface. Results are very similar to cases *a*, *b* and *d*, but they differ both qualitatively and quantitatively with the k-ω solution, which seems to damp the water movement.

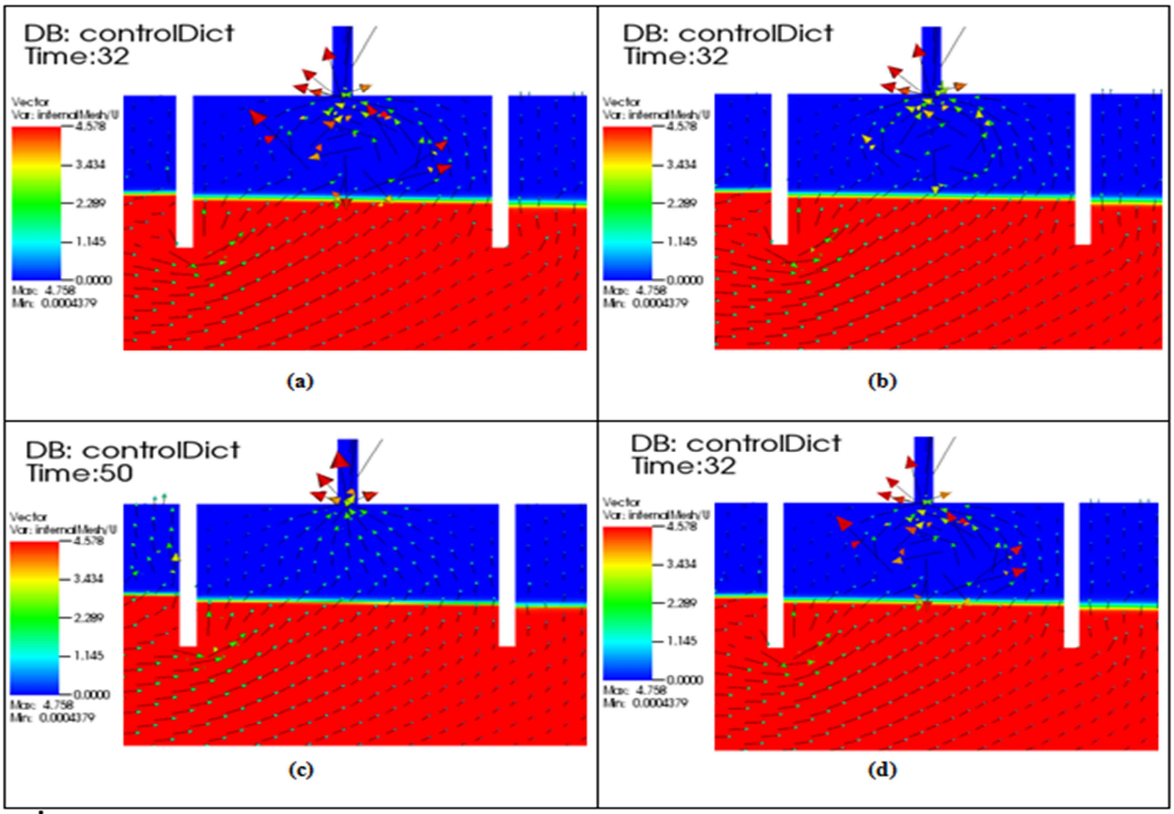

Figure 7. Velocity vectors at the first highest water raising surface: (a) Laminar, (b) k-ε, (c) k-ω and (d) Spalart Allmaras.

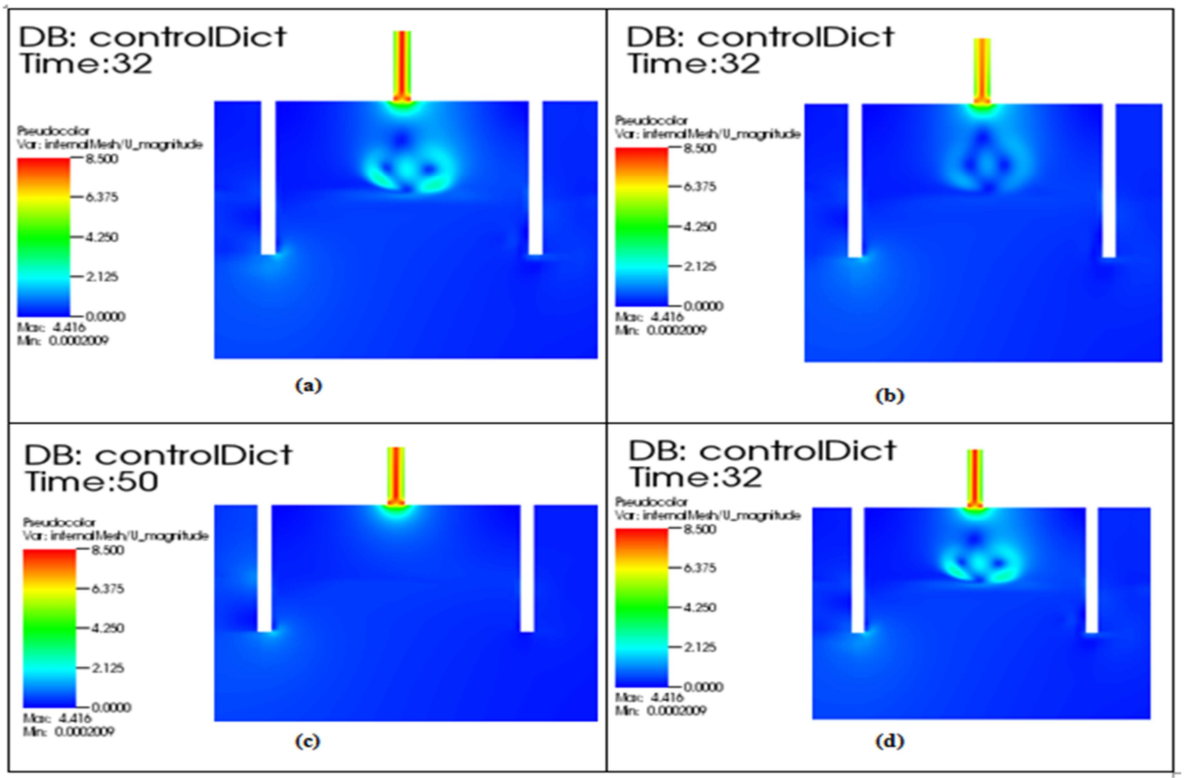

Figure 8. Velocity magnitude at the first highest water raising surface: (a) Laminar, (b) k-ε, (c) k-ω and (d) Spalart Allmaras.

As can be seen in Figs. 7 and 8, the velocity vectors, as well as the velocity magnitude of the Spalart Allmaras model are closer to the laminar model compared to the other models. This comparison is remarkable for the results shown in table 1.

4. CONCLUSIONS

Current paper presented a numerical simulation for a wave tank with an OWC device. It has been shown grid refinement test and an analytic verification for the laminar solution in a tank without the device. It was also shown a test for laminar and different turbulent flow models (k-ε, k-ω and Spalart Allmaras) for a tank with the OWC device. Results have shown that Spalart Allmaras model presented the greatest similarity to the laminar model, with the lowest difference attributed to the average water raising surface and the velocity field (vector and magnitude). In turn, the k-ω model presented the most discrepant results. It seems that in this model there is a viscosity addition, so much that there is a considerable softening of water raising surface.

5. ACKNOWLEDGMENTS

The author acknowledges the Coordenação de Aperfeiçoamento de Pessoal de Nível Superior (CAPES) and Conselho Nacional de Desenvolvimento Científico e Tecnológico for the financial support.

6. REFERENCES

Dean, R.G. and Dalrymple, R.A.. 1991. Water Wave Mechanics for Engineers & Scientists. World Scientific Pub Co Inc,.

FERRAZ, JULIANE GABINA ; NUNES, BRUNA RODRIGUES ; RODRIGUES, MICHEL KEPES ; BRUM, RUTH DA S. ; SOUZA, JEFERSON AVILA ; ROCHA, LUIZ ALBERTO OLIVEIRA ; ISOLDI, LIÉRCIO ANDRÉ ; DOS SANTOS, ELIZALDO DOMINGUES . Modelagem computacional de um trocador de calor solo-ar empregando diferentes modelagens para turbulência. Scientia Plena , v. 11, p. 10, 2015.

Henk Kaarle Versteeg, Weeratunge Malalasekera (2007). An Introduction to Computational Fluid Dynamics: The Finite Volume Method. Pearson Education Limited. ISBN 9780131274983.

Launder, B.E.; Spalding, D.B. (March 1974). "The numerical computation of turbulent flows". Computer Methods in Applied Mechanics and Engineering.:269–289. doi:10.1016/0045-7825(74)90029-2.

RAMIM, P.; PETIT, O.; e NILSSON, U. 2001. "Project Work: InterSettingFoam."

SOUZA, Jeferson Avila; SANTOS, Elizaldo Domingues dos; ISOLDI, Liércio André. Numerical simulation of an owc devise. In: COBEM - INTERNATIONAL CONGRESS OF MECHANICAL ENGINEERING, 22., 2013, Ribeirão Preto.

Thorpe, T. W. 1999. "An Overview Of Wave Energy Technologies: Status, Performance And Costs." 4° European Wave Energy Conference . Alborg, Denmark

7. RESPONSIBILITY NOTICE